A Deep Learning Framework for Breast Tumor Detection and Localization from Microwave Imaging Data

Salwa K. Al Khatib
ECE Department
Beirut Arab University
Beirut, Lebanon
salwa.alkhatib@ieee.org

Tarek Naous
ECE Department
American University of Beirut
Beirut, Lebanon
tnn11@aub.edu.lb

Raed M. Shubair
ECE Department
New York University
Abu Dhabi, UAE
raed.shubair@nyu.edu

Hilal M. El Misilmani
ECE Department
Beirut Arab University
Beirut, Lebanon
hilal.elmisilmani@ieee.org

***Abstract*—Breast Microwave Imaging (BMI) has emerged as a viable alternative to conventional breast cancer screening techniques due to its favorable features and a higher rate of detection. This paper presents a deep learning framework consisting of deep neural networks with convolutional layers to facilitate the process of tumor detection, localization, and characterization from scattering parameter measurements and metadata features. The developed deep learning framework outperforms other techniques in the literature in terms of detection accuracy, tumor localization, and characterization. The promising results of this paper demonstrate the potential and benefits of performing BMI via deep neural networks trained on practical scattering parameter measurements.**

***Index Terms*—Microwave Imaging, Deep Learning, Neural Networks, Breast Cancer Detection**

I. Introduction

Over the last few decades, predictive models have been widely utilized for detecting cancerous tumors such as breast cancer [1], which is the most common type of cancer among women worldwide [2]. Breast Microwave Imaging (BMI) has been an active area of research, showing promise as a non-ionizing technique for the early detection of breast tumors [3]. Upon illuminating the breast area with low-power microwave pulses, antennas positioned around the breast area collect the reflected signals for further pre-processing and image reconstruction via specific algorithms [4], [5]. While BMI systems have been extensively studied in the last two decades, limited work has investigated deep learning-based solutions for breast tumor detection and localization from the reflected signals in BMI systems. In [6], a dataset of microwave backscattered signals of generated 3D tumour models was used to train a support vector machine (SVM) classifier with a deep learning feature embedding to differentiate malignant and benign tumours. An accuracy of 93.44% was reached. Microwave mammogram apparatus clinical data was collected and pre-processed in [7] to train a classifier that detects breast lesions. A SVM with a quadratic kernel was trained using this data, where an accuracy of 97% was reached.

Recently, the University of Manitoba Breast Microwave Imaging Dataset (UM-BMID) was released in [8], where the authors developed a logistic regression model that detects the presence of a breast tumor based on the reflected S_{11} parameters. The authors achieved a detection accuracy of 85%. However, they did not make full use of the dataset which contains a larger number of scans with the reflected S_{21} parameters and several metadata features. In this work, we make full usage of the UM-BMID dataset and develop a deep learning framework consisting of several neural network models that can detect, localize, and characterize breast tumors based on S_{11} and S_{21} scattering parameters captured by the BMI system and various metadata features.

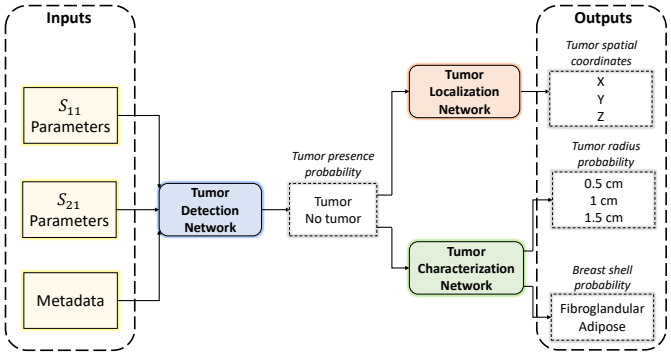

Fig. 1: Diagram of the proposed deep learning framework of several neural network models for tumor detection, localization, and characterization.

The rest of the paper is organized as follows: In Section II, we describe our proposed deep learning framework, starting with a description of the dataset used and followed by the deep neural network models developed. Section III analyses the results achieved by the neural network models of the proposed framework. Concluding remarks follow in Section IV.

II. Proposed Deep Learning Framework

We propose a deep learning framework for breast cancer screening using BMI as depicted in Figure 1. This framework starts with a tumor detection stage followed by two parallel

TABLE I: Selected metadata features from the dataset that were used in training the framework

Feature	Description	Used As
Bi-rads	BI-RADS density class of the phantom	Input
Ant-rad	The radial distance from the center of the imaging chamber of the SMA connector on the antennas	Input
Fib-ang	The polar angle of rotation of the fibroglandular shell	Input
Fib-x	The x-position of the center of the fibroglandular shell, with respect to the center of the adipose shell	Input
Fib-y	The y-position of the center of the fibroglandular shell, with respect to the center of the adipose shell	Input
Adi-x	The x-position of the center of the adipose shell	Input
Adi-y	The y-position of the center of the adipose shell	Input
Tum-rad	Radius of tumor used	Output
Tum-x	x-position of tumor	Output
Tum-y	y-position of tumor	Output
Tum-z	z-position of tumor	Output
Tum-in-fib	Indicates if the tumor was contained in the fibroglandular shell or the adipose shell	Output

stages of localization and characterization of the detected tumor.

A. Dataset

1) Description & Input-Output Features: We have exploited UM-BMID [8], an open-access experimental dataset containing scans of MRI-derived 3D-printed breast phantoms. The dataset is offered in two generations, where the first generation includes 249 scans of 13 phantoms and the second generation includes 1008 scans of 66 phantoms. The phantoms are made of unique adipose-fibroglandular shell combinations. In addition, the scans in the first generation contain only S_{11} parameters, while the second generation contains both S_{11} and S_{21} parameters along with additional metadata related to the phantoms and the tumor analogs. We use the second generation of the dataset which has not been previously explored. The selected features from the available metadata and their descriptions are shown in Table I.

2) Pre-processing: As a data preprocessing step, the scattering parameters were converted from the frequency domain to the time domain using the inverse discrete Fourier transform. A time window of $[0.71ns - 5.71ns]$ was applied, as suggested in [8], to ensure that the used parameters correspond to the responses to the phantoms only. This resulted in 35 responses for each one of the 72 antenna positions used in the scanning process. This necessitates the use of a convolutional layer as the input layer to avoid using an input layer with 2520 neurons, as required by a standard feed-forward neural network. Thus, the responses were stacked together in matrix form for each data sample. The absolute value of each sample was then taken, resulting in a 35×72 input matrix feature that represents one scan.

Additionally, the input features were normalized using the z-score approach as follows:

$$x' = \frac{x - \mu}{\sigma} \tag{1}$$

where x is an input sample, x' is the normalized samples, and μ and σ are the mean and standard deviation of the training samples.

B. Neural Network Models

1) Tumor Detection Network: This model is used in the first stage of the framework. It is a binary classification model which aims at detecting whether a tumor exists or not.

2) Tumor Localization Network: This model localizes the tumor in space. The predicted features include $tum-x$, $tum-y$, and $tum-z$, the coordinates of the tumor in centimeters, where the origin is the center of the imaging chamber.

3) Tumor Characterization Network: This model is a multi-task model with two objectives: the classification of the tumor into either the fibroglandular or the adipose shell of the breast phantom, and the classification of the radius of the tumor into 0.5 cm, 1.0 cm, or 1.5 cm (the three distinct radius classes used in UM-BMID).

The architectures of the aforementioned networks are shown in the combined illustration of Figure 2. All networks have similar input layers, where convolutional and max-pooling layers are used to extract features from matrices containing time-inverted scattering parameters. The input metadata features, as specified in Table I, are fed as a vector to a set of fully connected layers, of which the output is then concatenated with the flattened feature maps of the convolutional and pooling layers. The concatenated vector is then fed to a set of fully connected layers which are different for each network and were tuned for optimal test-set performance of each task. We use the Rectified Linear Unit (ReLU) activation function for all layers in the networks, except for the output layer of each network of which the activation functions are specified in Figure 2.

III. Experimental Results

A. Implementation

The neural network models are developed using the Keras deep learning library. The dataset is randomly partitioned into 80% training, 10% validation, and 10% testing using a random seed of 42. All models were trained and evaluated on the same data split using the Adaptive Moment Estimation (ADAM) optimization algorithm. For the tumor localization and characterization networks, only the scans where a tumor was present were included in the training, resulting in 504

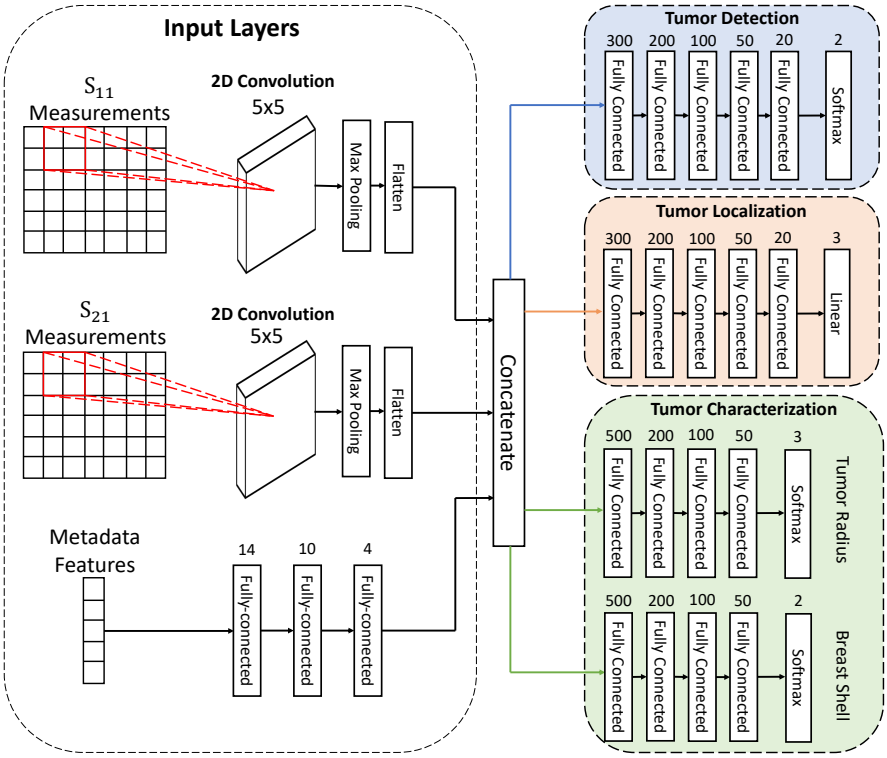

Fig. 2: Combined illustration of the neural network model architectures in the proposed framework. All networks have the same input layers. Output layer of each network is highlighted in a different color.

data samples to train these two networks. Our code is publicly available[1].

B. Numerical Evaluation

1) Evaluation Metrics: We evaluate classification tasks, namely tumor detection and characterization, using the F1 score measure, given by:

$$F1 = 2 * \frac{precision * recall}{precision + recall} \tag{2}$$

where the precision and recall measures are calculated from the True Positive (TP), False Positive (FP), and False Negative (FN) values as follows:

$$precision = \frac{TP}{TP + FP} \tag{3}$$

$$recall = \frac{TP}{TP + FN} \tag{4}$$

The regression task of tumor localization is evaluated using the Mean Squared Error (MSE) and the Coefficient of Determination (R^2) score measures. MSE is the average squared difference between the ouputs of the model and the ground truth values. It is obtained by the following:

$$MSE = \frac{1}{m} \sum_{i=1}^{m} (h(x_i) - y_i)^2 \tag{5}$$

[1]https://github.com/RFAD-Research-Team/breast-tumor-detection

where m is the number of samples in the test set, $h(x_i)$ is the predicted output of the model for a test sample x_i, and y_i is the ground truth value which is the actual value in the test set.

On the other hand, the R^2 score is expressed by:

$$R^2 = 1 - \frac{\sum_{i=1}^{m} (h(x_i) - y_i)^2}{\sum_{i=1}^{m} (y_i - y_{mean})^2} \tag{6}$$

where y_{mean} represents the mean of the ground truth values in the test set.

2) Training & Validation: Figure 3 shows the training and validation curves for the neural network models. The training and validation accuracy curves of the tumor detection network are plotted in Figure 3a. Both the training and validation curves surpassed the 90% mark. It can be noticed that both curves are close to each other, which indicates that no overfitting occurred. As for Figure 3b, it shows both the MSE and validation MSE curves of the tumor localization network, where a certain gap appears between them after the 40^{th} epoch. The training MSE falls below 0.2, while the validation MSE remains slightly above 0.2. Finally, Figure 3c presents the accuracy and validation accuracy curves of the tumor characterization network for both tasks: classifying the tumor radius and the breast shell in which the tumor resides. It is shown that, for the shell classification task, the model achieves high performance on both train and validation sets, reaching a value close to 100%. However, the model under-performs on the tumor radius classification task, where a substantial gap exists between the train and validation accuracy curves.

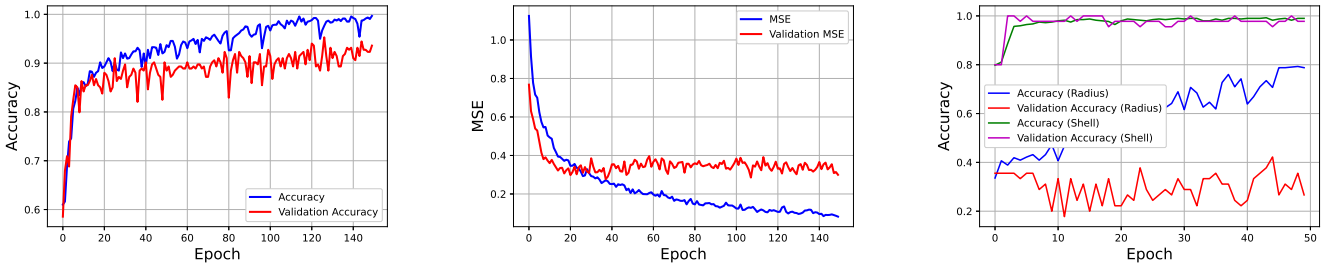

(a) Tumor Detection Network: Accuracy Curves

(b) Tumor Localization Network: MSE Curves

(c) Tumor Characterization Network: Accuracy Curves

Fig. 3: Training and Validation Curves of the Neural Network Models of the Proposed Deep Learning Framework

3) Test Set Evaluation: The results achieved by our proposed neural network models on the test set are summarized in Table II. For comparative analysis, we report the results achieved by each network when using different combinations of inputs, namely the S_{11} and S_{21} parameters, in addition to the metadata features.

The tumor detection model achieved an F1 score of 0.87 when trained using only S_{11} parameters. Adding the S_{21} parameters as an additional input increased the F1 score up to 0.92. A significant performance boost was also noticed by adding the metadata features, where the model reached a very high F1 score of 0.96, surpassing the results in [8].

In terms of tumor localization, the localization network reached the lowest MSE of 0.27 and the highest R^2 score of 0.75 when all input layers were used. Using all input features to train the model improved performance significantly compared with the cases of using only S_{11} or both S_{11} and S_{21}, where higher MSE and lower R^2 score was achieved.

A similar trend in the results is achieved by the tumor characterization network, where performance on tumor radius and breast shell classification reached an F1 score of 0.4 and 1.0 respectively. While the network was successful in classifying in which breast shell the tumor is present, performance was poor in identifying tumor radius, with the F1 score being low at 0.4. This may be due to the limited number of samples in the dataset with information on tumor radius, in addition to the high imbalance observed in the classes. Hence, this limitation will be subject to future investigation.

TABLE II: Numerical results achieved by the neural network models

Model		**Inputs**			**MSE**	R^2	**F1**
		S_{11}	S_{21}	**Metadata**			
Tumor Detection		✓			-	-	0.87
		✓	✓		-	-	0.92
		✓	✓	✓	-	-	**0.96**
Tumor Localization		✓			0.36	0.66	-
		✓	✓		0.34	0.67	-
		✓	✓	✓	**0.27**	**0.75**	-
Tumor Characterization	**Tumor Radius**	✓			-	-	0.27
		✓	✓		-	-	0.34
		✓	✓	✓	-	-	**0.4**
	Breast Shell	✓			-	-	0.97
		✓	✓		-	-	0.97
		✓	✓	✓	-	-	**1.0**

IV. Conclusion

This paper presented a deep learning framework for breast tumor detection, localization, and characterization from microwave imaging data. The framework consists of deep neural networks with convolutional layers that take time-inverted scattering parameters and several metadata features. The promising results of this paper demonstrate the potential and benefits of performing BMI via deep neural networks trained on practical scattering parameter measurements. Our future work will focus on learning better localization models from a small number of data samples.

References

[1] D. Bazazeh and R. Shubair, "Comparative study of machine learning algorithms for breast cancer detection and diagnosis," in *2016 5th international conference on electronic devices, systems and applications (ICEDSA)*, pp. 1–4, IEEE, 2016.

[2] R. L. Siegel, K. D. Miller, H. E. Fuchs, and A. Jemal, "Cancer statistics, 2021.," *CA: a cancer journal for clinicians*, vol. 71, no. 1, pp. 7–33, 2021.

[3] H. M. El Misilmani, T. Naous, S. K. Al Khatib, and K. Y. Kabalan, "A survey on antenna designs for breast cancer detection using microwave imaging," *IEEE Access*, vol. 8, pp. 102570–102594, 2020.

[4] D. O'Loughlin, M. O'Halloran, B. M. Moloney, M. Glavin, E. Jones, and M. A. Elahi, "Microwave breast imaging: Clinical advances and remaining challenges," *IEEE Transactions on Biomedical Engineering*, vol. 65, no. 11, pp. 2580–2590, 2018.

[5] E. Fear and M. Stuchly, "Microwave detection of breast cancer," *IEEE Transactions on Microwave Theory and Techniques*, vol. 48, no. 11, pp. 1854–1863, 2000.

[6] B. Gerazov and R. C. Conceicao, "Deep learning for tumour classification in homogeneous breast tissue in medical microwave imaging," in *IEEE EUROCON 2017-17th International Conference on Smart Technologies*, pp. 564–569, IEEE, 2017.

[7] S. P. Rana, M. Dey, G. Tiberi, L. Sani, A. Vispa, G. Raspa, M. Duranti, M. Ghavami, and S. Dudley, "Machine learning approaches for automated lesion detection in microwave breast imaging clinical data," *Scientific reports*, vol. 9, no. 1, pp. 1–12, 2019.

[8] T. Reimer, J. Krenkevich, and S. Pistorius, "An open-access experimental dataset for breast microwave imaging," in *2020 14th European Conference on Antennas and Propagation (EuCAP)*, pp. 1–5, IEEE, 2020.